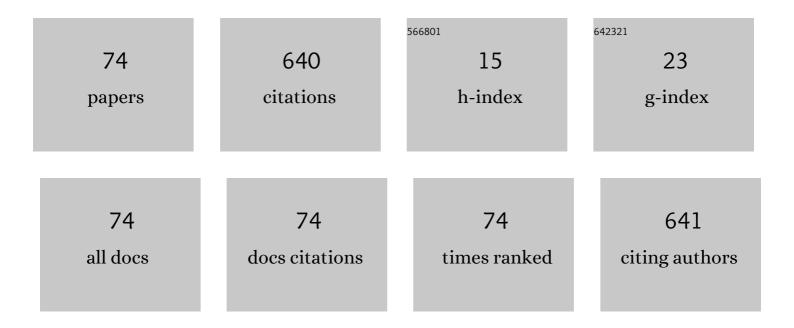
Toshimitsu Mochizuki

List of Publications by Year in descending order

Source: https://exaly.com/author-pdf/6805981/publications.pdf Version: 2024-02-01



#	Article	IF	CITATIONS
1	Integration of Si Heterojunction Solar Cells with III–V Solar Cells by the Pd Nanoparticle Array-Mediated "Smart Stack―Approach. ACS Applied Materials & Interfaces, 2022, 14, 11322-11329.	4.0	9
2	Instantaneous Photocarrier Transport at the Interface in Perovskite Solar Cells to Generate Photovoltage. Photonics, 2022, 9, 316.	0.9	2
3	Catalytic reduction and reductive functionalisation of carbon dioxide with waste silicon from solar panel as the reducing agent. Energy Advances, 2022, 1, 385-390.	1.4	3
4	Cu Nanoparticle Array-Mediated III–V/Si Integration: Application in Series-Connected Tandem Solar Cells. ACS Applied Energy Materials, 2020, 3, 3445-3453.	2.5	9
5	Effects of the Non-Radiative Recombination and Bandgap Reduction in Heat-Recovery Solar Cell. , 2020,		1
6	Impact of electrical shading loss suppression on interdigitated-back-contact Si solar cells with screen printing metallization concepts. AIP Conference Proceedings, 2019, , .	0.3	1
7	An Investigation of Internal Quantum Efficiency of Bifacial Interdigitated Back Contact (IBC) Crystalline Silicon Solar Cell. IEEE Journal of Photovoltaics, 2019, 9, 1526-1531.	1.5	7
8	Noncontact evaluation of electrical passivation of oxidized silicon using laser terahertz emission microscope and corona charging. Journal of Applied Physics, 2019, 125, .	1.1	13
9	Heat-Recovery Solar Cell. Physical Review Applied, 2019, 12, .	1.5	3
10	A concept of nonequilibrium solar cell heat recovery solar cell. , 2019, , .		0
11	Coherent detection of THz-induced sideband emission from excitons in the nonperturbative regime. Physical Review B, 2018, 97, .	1.1	3
12	Evaluation of carrier collection probability in bifacial interdigitated-back-contact crystalline silicon solar cells by the internal quantum efficiency mapping method. Japanese Journal of Applied Physics, 2018, 57, 040315.	0.8	6
13	A solar cell enabling heat recovery without fast carrier extraction. , 2018, , .		2
14	Bifacial interdigitated-back-contact (IBC) crystalline silicon solar cell: fabrication and evaluation by internal quantum efficiency mapping. , 2018, , .		6
15	Nonequilibrium Theory of the Conversion Efficiency Limit of Solar Cells Including Thermalization and Extraction of Carriers. Physical Review Applied, 2018, 10, .	1.5	12
16	Internal quantum efficiency mapping for evaluation of rear surface of passivated emitter and rear cell. Applied Physics Express, 2018, 11, 086601.	1.1	3
17	Anomalous Metal Phase Emergent on the Verge of an Exciton Mott Transition. Physical Review Letters, 2017, 118, 067401.	2.9	18
18	Internal quantum efficiency mapping analysis for a >20%-efficiency n-type bifacial solar cell with front-side emitter formed by BBr3 thermal diffusion. Japanese Journal of Applied Physics, 2017, 56, 102303.	0.8	4

Тознімітѕи Мосніzикі

#	Article	IF	CITATIONS
19	Effects of different particle-sized Al pastes on rear local contact formation and cell performance in passivated emitter rear cells. Energy Procedia, 2017, 124, 412-417.	1.8	9
20	Probing the surface potential of oxidized silicon by assessing terahertz emission. Applied Physics Letters, 2017, 110, .	1.5	30
21	High-efficiency III–V//Si tandem solar cells enabled by the Pd nanoparticle array-mediated "smart stack― approach. Applied Physics Express, 2017, 10, 072301.	1.1	34
22	Subcycle control of optical response by using a terahertz excitonic dressed state. , 2017, , .		0
23	Calibration standards and measurement accuracy of absolute electroluminescence and internal properties in multi-junction and arrayed solar cells. Proceedings of SPIE, 2016, , .	0.8	3
24	Subcycle Optical Response Caused by a Terahertz Dressed State with Phase-Locked Wave Functions. Physical Review Letters, 2016, 117, 277402.	2.9	29
25	Solar-cell radiance standard for absolute electroluminescence measurements and open-circuit voltage mapping of silicon solar modules. Journal of Applied Physics, 2016, 119, .	1.1	24
26	Current leakage and fill factor in multi-junction solar cells linked via absolute electroluminescence characterization. , 2016, , .		2
27	A "smart stack―triple-junction cell consisting of InGaP/GaAs and crystalline Si. , 2016, , .		6
28	Phase-sensitive observation of THz-dressed exciton. , 2016, , .		0
29	Conversion efficiency limits and bandgap designs for multi-junction solar cells with internal radiative efficiencies below unity. Optics Express, 2016, 24, A740.	1.7	34
30	Characterizations of Radiation Damage in Multijunction Solar Cells Focused on Subcell Internal Luminescence Quantum Yields via Absolute Electroluminescence Measurements. IEEE Journal of Photovoltaics, 2016, 6, 777-782.	1.5	25
31	Characterization and modeling of radiation damages via internal radiative efficiency in multi-junction solar cells. Proceedings of SPIE, 2016, , .	0.8	3
32	Evaluation of Si-SiOx Interface using Laser Terahertz Emission Microscope (LTEM). , 2016, , .		0
33	Time-resolved observation of coherent excitonic nonlinear response with a table-top narrowband THz pulse wave. Applied Physics Letters, 2015, 107, 221106.	1.5	15
34	Analysis of Oxyluciferin Photoluminescence Pathways in Aqueous Solutions. Photochemistry and Photobiology, 2015, 91, 74-83.	1.3	12
35	Characterizations of radiation damages in multi-junction solar cells focused on subcell internal luminescence quantum yields via absolute electroluminescence measurements. , 2015, , .		0
36	Absolute electroluminescence imaging of multi-junction solar cells and calibration standards. , 2015, , .		10

3

Тознімітѕи Мосніzикі

#	Article	IF	CITATIONS
37	Thorough subcells diagnosis in a multi-junction solar cell via absolute electroluminescence-efficiency measurements. Scientific Reports, 2015, 5, 7836.	1.6	74
38	Effect of very high magnetic field on the optical properties of firefly light emitter oxyluciferin. Journal of Luminescence, 2015, 165, 15-18.	1.5	2
39	Time-resolved observation of excitonic dynamics under coherent terahertz excitation in GaAs quantum wells. , 2015, , .		0
40	Multi-junction-solar-cell designs and characterizations based on detailed-balance principle and luminescence yields. Proceedings of SPIE, 2015, , .	0.8	2
41	Mode imaging and loss evaluation of semiconductor waveguides. Review of Scientific Instruments, 2014, 85, 053109.	0.6	0
42	Conversion efficiency limits and optimized designs for tandem solar cells with realistic sub-cell material quality. , 2014, , .		2
43	Balance sheets of energy and carriers and subcell characteristics in a GaInP/GaAs/Ge tandem solar cell. , 2014, , .		0
44	Robust red-emission spectra and yields in firefly bioluminescence against temperature changes. Applied Physics Letters, 2014, 104, .	1.5	23
45	Gain switching of a double-core-waveguide semiconductor laser via traveling-wave optical pumping. Applied Physics Express, 2014, 7, 062701.	1.1	Ο
46	Analysis of Photoexcitation Energy Dependence in the Photoluminescence of Firefly Luciferin. Photochemistry and Photobiology, 2014, 90, 820-828.	1.3	4
47	Impact of sub-cell internal luminescence yields on energy conversion efficiencies of tandem solar cells: A design principle. Applied Physics Letters, 2014, 104, 031118.	1.5	28
48	Terahertz-Induced Optical Emission of Photoexcited Undoped GaAs Quantum Wells. Physical Review Letters, 2013, 111, 067401.	2.9	16
49	Electroluminescence of GaNAs/GaAs MQWs p–i–n junctions grown by RF-MBE using modulated nitrogen radical beam source. Journal of Crystal Growth, 2013, 378, 150-153.	0.7	3
50	Intrinsic radiative lifetime derived via absorption cross section of one-dimensional excitons. Scientific Reports, 2013, 3, 1941.	1.6	6
51	Gain-switched pulses from InGaAs ridge-quantum-well lasers limited by intrinsic dynamical gain suppression. Optics Express, 2013, 21, 7570.	1.7	19
52	Transient hot-carrier optical gain in a gain-switched semiconductor laser. Applied Physics Letters, 2013, 103, .	1.5	14
53	Biexciton emission from single isoelectronic traps formed by nitrogen-nitrogen pairs in GaAs. , 2013, , .		0
54	Double-Core-Slab-Waveguide Semiconductor Lasers for End Optical Pumping. Applied Physics Express, 2013, 6, 062702.	1.1	2

4

Тознімітѕи Мосніzикі

#	Article	IF	CITATIONS
55	Photoluminescence flash induced by intense single-cycle terahertz pulses in undoped GaAs quantum wells. , 2013, , .		0
56	Fluorescent Radiation Thermometry at Cryogenic Temperatures Based on Detailed Balance Relation. Applied Physics Express, 2013, 6, 056602.	1.1	1
57	High-power THz pulse generation and nonlinear THz spectroscopy. , 2013, , .		Ο
58	Waveguide Two-Point Differential-Excitation Method for Quantitative Absorption Measurements of Nanostructures. Japanese Journal of Applied Physics, 2012, 51, 106601.	0.8	1
59	Analysis of Gain-Switching Characteristics Including Strong Gain Saturation Effects in Low-Dimensional Semiconductor Lasers. Japanese Journal of Applied Physics, 2012, 51, 098001.	0.8	8
60	Observation of high Rydberg states of one-dimensional excitons in GaAs quantum wires by magnetophotoluminescence excitation spectroscopy. Physical Review B, 2012, 86, .	1.1	14
61	Biexciton Luminescence from Individual Isoelectronic Traps in Nitrogen \$delta\$-Doped GaAs. Applied Physics Express, 2012, 5, 111201.	1.1	8
62	Electrical and Optical Properties of GaNAs/GaAs MQW p-i-n Junction. Transactions of the Materials Research Society of Japan, 2012, 37, 193-196.	0.2	1
63	Waveguide Two-Point Differential-Excitation Method for Quantitative Absorption Measurements of Nanostructures. Japanese Journal of Applied Physics, 2012, 51, 106601.	0.8	1
64	Magnetotransport in adsorbate-induced two-dimensional electron systems on cleaved InAs surfaces. Journal of Applied Physics, 2011, 109, 102416.	1.1	10
65	Evidence for spin-glass ordering in submonolayer Fe films on InAs. , 2010, , .		0
66	Alkali Metal Induced Two Dimensional Electron Systems at Cleaved Surfaces of InAs. , 2010, , .		0
67	Quantum Hall effect at cleaved surfaces of InAs and InSb. Physica E: Low-Dimensional Systems and Nanostructures, 2008, 40, 1030-1033.	1.3	1
68	Evidence for Two-Dimensional Spin-Glass Ordering in Submonolayer Fe Films on Cleaved InAs Surfaces. Physical Review Letters, 2008, 101, 267204.	2.9	20
69	Alkali-metal-induced Fermi-level and two-dimensional electrons at cleaved InAs(110) surfaces. Physical Review B, 2008, 77, .	1.1	6
70	Quantum Hall effect at cleaved InSb surfaces and low-temperature annealing effect. Applied Physics Letters, 2007, 90, 202104.	1.5	17
71	Magnetotransport of Two-dimensional Electrons at In-situ Cleaved InAs Surfaces. AIP Conference Proceedings, 2007, , .	0.3	0
72	Observation of the quantum Hall effect in cleaved InAs surfaces. Physica E: Low-Dimensional Systems and Nanostructures, 2006, 34, 156-159.	1.3	2

#	Article	IF	CITATIONS
73	Two-dimensional electrons at a cleaved semiconductor surface: Observation of the quantum Hall effect. Applied Physics Letters, 2005, 87, 062103.	1.5	15
74	Single Photon Generation from Nitrogen Atomic-Layer Doped Gallium Arsenide. Materials Science Forum, 0, 706-709, 2916-2921.	0.3	2